Experimental Study on Factors that Influence the Diameter of Dry Granulated Particles

TONG Lige[1,2*], ZHANG Pei[1], YIN Shaowu[1,2], LIU Yongxu[1], WANG Li[1,2], DING Yulong[3]

1. School of Mechanical Engineering, University of Science & Technology Beijing, Beijing 100083, China
2. Beijing Engineering Research Center for Energy Saving and Environmental Protection, University of Science and Technology Beijing, Beijing 100083, China
3. School of Chemical Engineering, University of Birmingham, Birmingham B152TT, United Kingdom

The development of heat recovery methods for dry granulation processes from blast furnace slag in the iron and steel industry is limited because of the high consumption of granulation energy during these processes. To determine the factors that influence the diameter of granulated particles, a paraffin test platform for gas quenching granulation was established. The influences of air velocity, air flow rate, liquid mass flow rate, and liquid pipe diameter on the final particle size and mass distribution were studied. Experimental results showed that the final particle size decreased (from 1.07 mm to 0.81 mm) with increasing air velocity (from 28.3 m/s to 113.2 m/s). However, when air velocity was higher than 60 m/s, its influence on particle diameter decreased significantly. The experimental data were analyzed using SPSS Statistics software, which indicated that the effect of air velocity on particle diameter was the most significant, followed by those of air flow and liquid pipe diameter. The effect of liquid mass flow was the least significant.

Keywords: blast furnace slag, simulation test, granulation, gas quenching

Introduction

Blast furnace slag produced during iron-making processes is quickly quenched with water to form glassy particles. These particles can be used as an alternative material for Portland cement. In the wet granulation process, the waste heat of molten slag discharged at high temperatures ranging from 1450°C to 1650°C is typically unrecovered. Simultaneously, a large amount of water is consumed, and waste gas, including sulfide, is discharged into the ambient environment. Dry granulation for molten slag has recently received considerable attention because of environmental and energy recovery considerations. In the dry granulation process, molten slag is granulated into particles, and the waste energy of slag can be recovered to generate steam or heated air in fluidized or moving beds [1-2]. Recently, dry granulation methods for blast furnace slag are classified based on different crushing approaches for molten slag as follows: roller drum method, gas quenching method (GQM), rotor centrifugal granulation method, and mechanical stirring method [3-5]. The relatively low heat conductivity of most silicate slags causes difficulties in recovering energy contained in liquid slag. Thus, most of these methods result in unsatisfactory heat recycling efficiency and undesired properties for secondary applications in other processes [6].

Gas quenching granulation is a promising process because the diameter of slag particles can be controlled to

Lige Tong: Assistant Professor

This study is supported by the National Natural Science Foundation of China (Grant No. 51206010) and the National Basic Research Program of China (973 Program) (Grant No. 2012CB720406).

remain extremely small, and thus, suitable for efficient heat recovery, thereby fulfilling the requirement for practical application. In the gas quenching process, high-speed and high-pressure gas is used to impinge the stream of molten slag, during which slag is broken down into tiny particles with rapid cooling [7]. Liu *et al*. [8] performed a theoretical analysis on transient air cooling and the solidification behavior of a spherical molten slag particle using a temperature model. They found that the solidification process accelerated with decreasing particle size. Furthermore, the solidification and heat transfer of an air-cooled molten blast furnace slag droplet was numerically simulated by Qiu *et al*. [9] using the volume of fluid method coupled with the solidification/melting model. They found that solidification time increased 2.29 times when particle diameter was increased by 1 order under the simulated conditions.

In industrial applications, the fast solidification of slag particles corresponds to a high heat recovery rate. Moreover, slag with a high cooling speed has a high proportion of glassy phase, which is conducive to its subsequent use. However, a small broken particle size corresponds to increased energy consumption in the gas quenching process. Thus, the gas quenching process requires a good control scheme to achieve a desired particle diameter distribution.

Current published research on the shearing breakup of liquid droplets in a gas medium has mainly focused on the effects of the Weber number (*We*), Reynolds number (*Re*), and Ohnesorge number (*Oh*) on the droplet diameter; several experimental correlations for predicting the droplet diameter have been established [10-12]. However, further research is required on problems in practical applications, such as the effect of controllable parameters on particle diameter in engineering applications. A few scholars have studied the gas quenching process for steel slag. The relationship among average particle diameter, superheat degree, steel slag basicity, ferrous oxide reduction value, ferric oxide added value, and unit air consumption has been obtained [13]. Other scholars have conducted experiments on slag granulation via GQM; they have found that the size distribution of steel slag after granulation is inversely proportional to gas pressure/flow rates and airflow velocity [14]. However, a few studies have focused on particle size control of blast furnace slag in the gas quenching process. Some scholars have confirmed the feasibility of the experimental simulation of blast furnace slag with paraffin; they have investigated the influences of rotating speed and mass flow rate on granule diameter and its mass distribution [15].

In the current study, paraffin was applied to simulate cold gas quenching for the granulation of blast furnace slag. Parameters for the size of the broken slag were obtained by building a gas quenching granulated bench. Various factors that affected average particle diameter, including air velocity, air flow, liquid mass flow rate, and liquid column diameter, were investigated. The relative importance of these factors was also identified to provide guidance for adjustment schemes to control the size of broken slag.

Gas quenching granulation setup

Materials

High-temperature molten slag is a non-Newtonian fluid and a mixture. A liquid column is granulated under the action of a high-velocity air stream in the gas quenching process, which is accompanied by a phase transition from liquid to solid. Glycerol, paraffin, aluminum, or other materials may be used to replace the molten slag in the experiment given that the diameter of the granulated particles depends minimally on temperature [16]. The natural physical properties of paraffin, aluminum, glycerol, and blast furnace slag are listed in Tab. 1. Glycerol is liquid at room temperature and has a low melting point. The melting point of aluminum is relatively high, which is difficult to attain. However, the melting point of paraffin is lower than those of the other materials. Paraffin is solid at room temperature and can be melted at 57–68°C. Therefore, achieving a solid–liquid–solid transition is relatively easy under laboratory conditions.

In the low-temperature section, the viscosity of molten slag decreases rapidly with increasing temperature (Fig.1). The viscosity-temperature correlation reaches a turning point at approximately 1347°C, beyond which the change trend of viscosity is flatter with temperature. That is, slag is initially a non-Newtonian fluid below the turning point temperature and then becomes a Newtonian fluid above this point. Fig.2 shows the relationship between temperatures and the viscosity of paraffin. When the temperature is below 70°C, the viscosity of paraffin is not a single function of temperature, and the viscosity-temperature curve is radial. Under such conditions, paraffin is a non-Newtonian fluid. When the temperature is higher than 70°C, the viscosity of paraffin does not change with shear rate and the viscosity is a single function of temperature. Thus, paraffin is a Newtonian fluid. In summary, blast furnace slag and paraffin have similar viscosity-temperature characteristics in the low-temperature section. Both materials demonstrate the characteristics of a non-Newtonian fluid. In an actual production process, blast furnace slag is granulated and rapidly cooled in air, and thus, demonstrates viscosity characteristic in the low-temperature section. In the experiment, we control the temperature of the paraffin in the low-

temperature section. Therefore, using paraffin to simulate the gas quenching granulation process of blast furnace slag is reasonable.

Table 1 Physical properties of the materials for analog

Materials	Density (kg/m^3)	Melting point (°C)
paraffin	860-905	57-68
glycerol	1260	17.8
aluminum	2700	660.4
blast furnace slag	2800-3200	1300

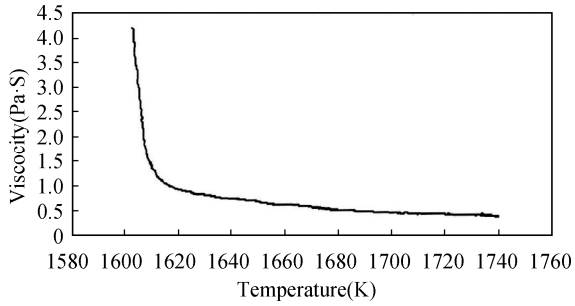

Fig. 1 Relationship between temperature and the viscosity of blast furnace slag [17]

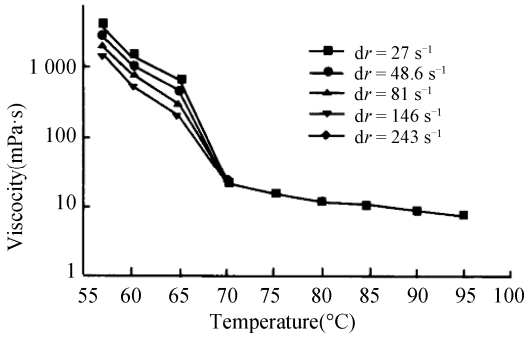

Fig. 2 Relationship between temperatures and the viscosity of paraffin [18]

Experimental setup

As shown in Fig.3, the experimental apparatus consists of four parts, namely, the melting, piping, gas quenching and collecting parts.

(a) Melting part

The paraffin box was wrapped in cotton insulation. Solid paraffin was initially placed in the paraffin box and melted using electric heating rods to melt. The melting point range of selected No. 58 paraffin is 58.0−60.0°C. During the experiment, the temperature of the liquid paraffin was maintained at approximately 60°C using the control system at about 60°C.

(b) Piping part

Downstream of the paraffin box, a series of piping components was used to control the diameter of liquid paraffin, including a paraffin box made of welded steel, a ferrule valve, ferrule adjustable joints, and a ferrule tee from top to bottom. The ferrule valve controlled the flow of liquid paraffin, and the ferrule adjustable joints changed the pipeline diameter to change the velocity and mass flow of liquid paraffin. As the liquid paraffin flowed through the piping part, the temperature declined. A thermocouple installed in the tee was used to measure the temperature of the liquid. Furthermore, a heating wire was wrapped around the pipe to prevent the paraffin from solidifying during the experiment. Heating power could be adjusted via a regulator.

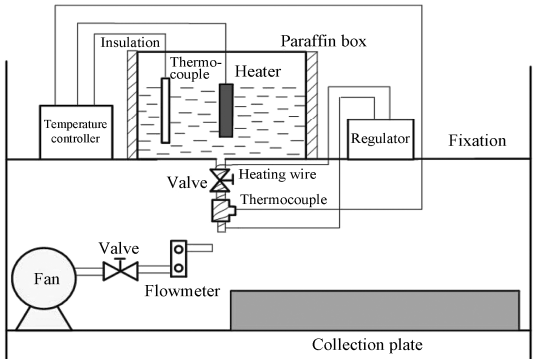

Fig. 3 Experimental flowchart of paraffin gas quenching granulation

(c) Gas quenching part

In the gas quenching part, air was supplied from a fan and air flow was controlled via a valve. Flow rate was measured using a gas flow meter. At the end of the air duct, a nozzle was installed to blow air into the melted paraffin column. Given that air velocity is the ratio of volume flow to the cross-sectional area of the outlet pipe, it can be adjusted by using gas quenching nozzles with varying diameters under the same air flow conditions.

(d) Collecting part

The experiment was conducted 2 m above the ground. Thus, the area where the granulated particles were scattered was relatively large. A plastic film was laid on the ground to serve as the collecting plate.

Calculation of granulated particle size distribution

Granulated particles collected on the collecting plate were classified using a circular sieve into five groups based on their diameter: 2−3 mm, 1.5−2 mm, 1−1.5 mm, 0.5−1 mm, and <0.5 mm. Then, the particles were weighed separately for each grade to obtain a mass percentage in all the particles. For each experiment, the col-

lected particles were sorted and weighed thrice. For each sorting, the average diameter was calculated using eq. 1. The final result (i.e., average diameter) of the experiment was the average of the calculated average diameters for three sortings.

$$d_{pj} = \frac{\sum_{j=1}^{n} \Delta p_j \overline{d_j}}{\sum_{j=1}^{n} \Delta p_j} \quad (1)$$

where $\overline{d_j}$ is the average diameter of each particle series, and $\overline{d_j} = (d_{j+1} + d_j)/2$; Δp_j is the percentage of each particle series in total mass.

Analysis and discussion of results

Effects of air velocity

As shown in Fig.4, when the temperature of liquid paraffin (t) is 60°C, its mass flow (q) is 5.78 g/s, and the diameter of the liquid column of paraffin (d) is 8 mm. In addition, the average diameter of the paraffin particles decreases with an increase in air velocity. However, the effect of air velocity varies significantly depending on the velocity magnitude. Consequently, the results are presented in two stages. In the first stage, air velocity (v) ranges from 30 m/s to 60 m/s. During this stage, the effect of air velocity on the average particle diameter is significant, and the curve that represents their relationship is approximately linear. In the second stage, air velocity is greater than 60 m/s. During this stage, the effect of air velocity on the average particle diameter becomes weak and gradually levels off.

These results are attributed to the fact that the impact force of air flow on liquid paraffin increases with air velocity, which reduces the average diameter of the gas quenching paraffin particles. When the liquid mass flow rate is constant, an increasing number of droplets are formed because of the small particle diameter. As shown in Fig. 2, when the paraffin is below 70°C, viscosity is significantly affected by temperature. The cooling effect of air flow on the liquid paraffin becomes stronger with the increase in air velocity. Subsequently, the speed of the solid-liquid phase interface movement of the paraffin becomes increasingly faster. Viscosity increases significantly at a low temperature, and droplets are less likely to be broken. Therefore, the increasing air velocity does not only promote breakage in the gas quenching liquid paraffin, but also inhibits secondary crushing, thereby weakening its granulation effect. Consequently, the curve begins to level off as air velocity increases.

The relationship between the particle size distribution of granulated paraffin and air velocity is shown in Fig.5. The average size of a broken particle is 0.8 mm when air velocity is 113.2 m/s. Most of the granulated particles are small. Those with a diameter of <1 mm account for over 70% of the particles. The proportion of particles with a diameter of >1 mm gradually increases with the decrease in air velocity. The average size of a broken particle is 1.06 mm when air velocity is 28.3 m/s. In this case, the ratio of particles with a diameter of >1 mm reaches approximately 50%.

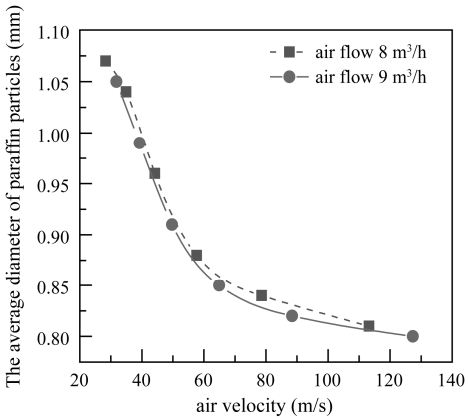

Fig. 4 Relationship between air velocity and the average diameter of paraffin particles (t = 60°C, q = 5.78 g/s, d = 8 mm)

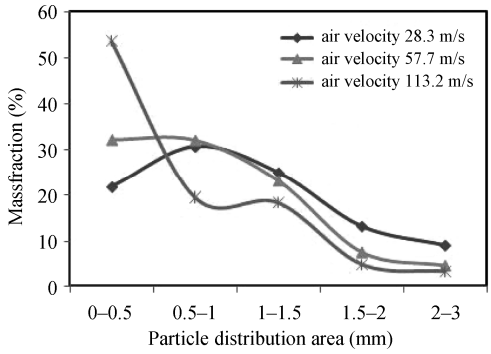

Fig. 5 The paraffin particle size distributions under different air velocities (t = 60°C, q = 5.78 g/s, d = 8 mm, q_v = 8 m³/h)

Effects of gas-liquid mass ratio

Before studying the influence of the gas-liquid mass ratio on the average diameter of gas quenching particles, we first examined the relationship between the average particle diameter and the air flow or mass flow rates of liquid paraffin. As shown in Fig. 6, the average diameter of paraffin particles decreases with an increase in the air flow.

However, the curve gradually levels off with increasing air flow. These results are attributed to the increase in

the impact force of air on liquid paraffin with air flow, and the average diameter of the gas quenching paraffin particles becoming smaller. By contrast, the cooling effect of air flow on the liquid paraffin increases with air flow. Such increase suppresses secondary crushing of liquid paraffin. The viscosity of paraffin also increases, and droplets become more difficult to break. Consequently, the granulation effect is weakened.

As shown in Fig. 7, the average diameter of paraffin particles increases with the mass flow rate of the paraffin, and the average diameter of the particles varies with the mass flow rate of paraffin, thereby presenting an approximately linear relationship.

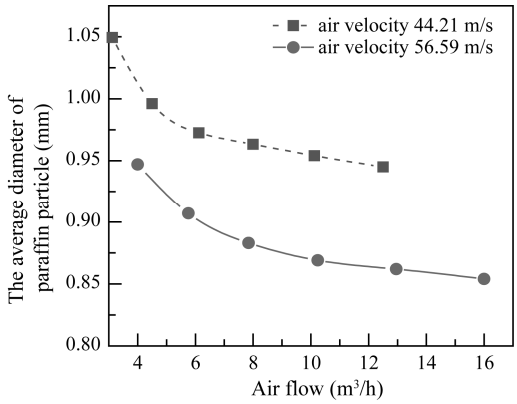

Fig. 6 Relationship between air flow and the average diameter of paraffin particles (t = 60°C, q = 5.78 g/s, d = 8 mm)

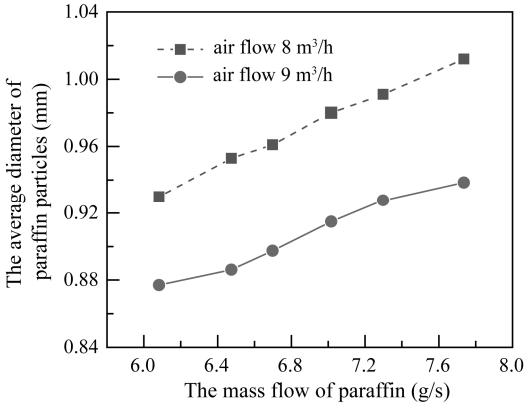

Fig. 7 Relationship between the mass flow of paraffin and the average diameter of paraffin particles (t = 60°C, d = 8 mm)

At room temperature, the density of air (ρ_g) is 1.205 kg/m^3, and the mass flow rate of air is the product of the air flow (q_v) and the density of air (ρ_g). Therefore, gas-liquid mass ratio G can be calculated using eq. (2) by dividing the mass flow rate of liquid paraffin q.

$$G = \rho_g q_v / q \tag{2}$$

As shown in Fig.8, the average diameter of paraffin particles obtained decreases with an increase in the gas-liquid mass ratio. These results are attributed to the increased impact force of air on unit mass of liquid paraffin with an increase in the gas-liquid mass ratio. The average diameter of the gas quenching paraffin particles is reduced with an increase in the droplet formation.

Gas quenching is an energy conversion process in which the kinetic energy of gas is converted into the surface energy, kinetic energy, and other forms of energy of the liquid paraffin. Higher air velocity or air flow corresponds to greater kinetic energy of the entering gas. Therefore, more energy can be converted into the surface energy of the liquid paraffin. This energy can be increased when the temperature and mass flow rate of the liquid paraffin and other conditions are constant, if the surface tension of the liquid paraffin is unchanged, and when only the surface area of the liquid paraffin increases. The surface area can be increased when the density and mass of the paraffin are the same, and only the diameter of the liquid paraffin droplets is reduced.

Fig. 9 shows the relationship between the particle size distribution of granulated paraffin and gas–liquid mass ratio. The average particle diameter is 0.941, 0.904, and 0.82 mm when gas–liquid mass ratio is 0.23, 0.59, and 0.93, respectively.

As shown in Fig. 9, the proportion of small particles is gradually reduced with decreasing gas–liquid mass ratio, whereas the proportion of large particles gradually increases. That is, the diameter of granulated particles increases as gas–liquid mass ratio is reduced.

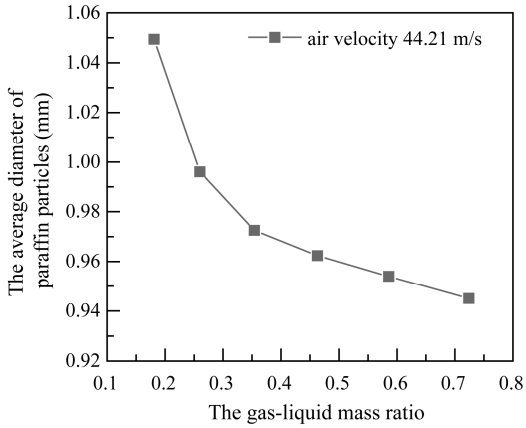

Fig. 8 Relationship between gas-liquid mass ratio and the average diameter of paraffin particles (t = 60°C, d = 8 mm, v = 44.21 m/s)

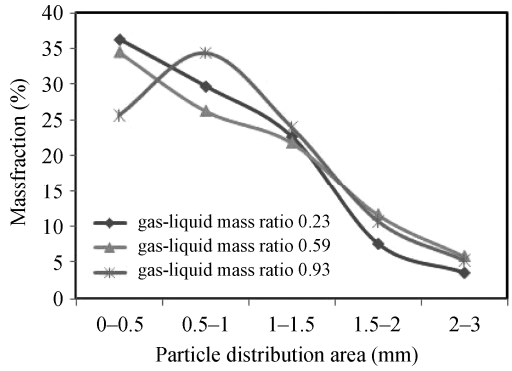

Fig. 9 The particle size distributions of the paraffin under different gas-liquid mass ratios (t = 60°C, d = 8 mm, v = 56.59 m/s)

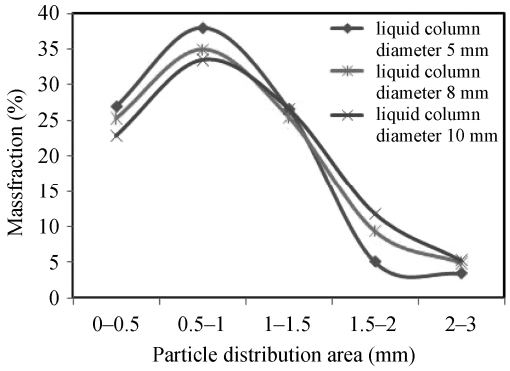

Fig. 11 The particle size distributions of the paraffin under different liquid column diameters (t = 60°C, q = 7.5 g/s, q_v = 8 m^3/h, v = 44.21 m/s)

Effects of liquid column diameter

As shown in Fig.10, the average diameter of the granulated particles gradually increases with the increase in paraffin liquid column diameter, and the relationship between liquid column diameter and gas quenching particle diameter is approximately linear.

Fig. 11 shows the relationship between the particle size distribution of crushed paraffin and liquid column diameter. The average particle diameter is 0.8702 mm when the liquid column diameter is 5 mm when most of the particles obtained after crushing are small. The proportion of particles with a diameter of <1.5 mm reached approximately 90%. The proportion of small particles decreases, whereas the proportion of large particles increases, with an increase in the diameter of the paraffin liquid column. The average size of broken particles is 0.99 mm when the liquid column diameter is 10 mm. In this case, the ratio of particles with a diameter of >1 mm reaches over 40%. That is, the diameter of granulated particles increases with that of the paraffin liquid column.

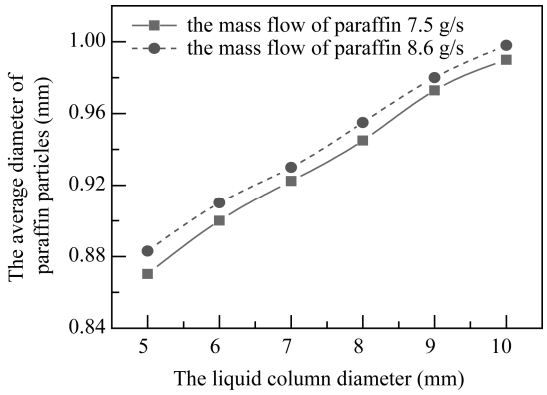

Fig. 10 Relationship between liquid column diameter and the average diameter of paraffin particles (t = 60°C, v = 44.21 m/s, qv = 8 m^3/h)

Order of importance of various factors that affect the broken particle size

On the basis of the preceding analysis, and within the scope of the study, the relationships of air flow, paraffin mass flow, and liquid column diameters with granulation size are approximately linear. The relationship between granulation size and air velocity is approximately linear in the air velocity ranges of less than 60 m/s and greater than 60 m/s.

The linear regression analysis of the experimental data was conducted using SPSS software for two air velocity ranges, i.e., wind speeds of less than 60 m/s and greater than 60 m/s. In the analysis, granulation diameter was used as the dependent variable, whereas air flow, air velocity, paraffin mass flow, and liquid column diameter were used as independent variables. The results are presented in Table 2 and Table 3.

In the “standard coefficient” column in Table 2 and Table 3, the absolute value of the coefficient of each variable reflects the strength of influence on particle diameter. When air velocity is less than 60 m/s, the factors are ordered as follows according to strength: air velocity > liquid column diameter > air flow > paraffin mass flow. When the velocity is greater than 60 m/s, the factors are ordered as follows according to strength: air velocity > air flow > liquid column diameter > paraffin mass flow.

Regardless of the range of air velocity, the effects of air velocity and paraffin mass flow on particle diameter are the strongest and the weakest, respectively. The effects of air flow and liquid column diameter are in between. The order of the effects of liquid column diameter and air flow is interchangeable at different intervals, but their standardized coefficient difference is small. Hence, the effects of these two factors are considered nearly the same.

In summary, the effect of air velocity on particle diameter is the most significant, followed by those of air

Table 2 Linear regression analysis when the wind speed is less than 60 m/s

	Non-standardized coefficient	Standard error	Standard coefficient	*t*	significance
	1.121	0.088		12.677	0.000
Air velocity	-0.005	0.001	-0.698	-7.096	0.000
Air flow	-0.010	0.002	-0.392	-4.223	0.001
Mass flow	-0.008	0.007	-0.109	-1.101	0.286
Diameter of liquid column	0.026	0.006	0.425	4.630	0.000

a. Dependent Variable: broken particle size

Table 3 Linear regression analysis when the wind speed is more than 60 m/s

	Non-standardized coefficient	Standard error	Standard coefficient	*t*	significance
	0.879	0.071		12.330	0.000
Air velocity	-0.002	0.000	-0.667	-6.619	0.000
Air flow	-0.010	0.002	-0.522	-6.337	0.000
Mass flow	0.006	0.007	0.086	0.824	0.429
Diameter of liquid column	0.024	0.004	0.510	6.157	0.000

a. Dependent Variable: broken particle size

flow and liquid pipe diameter, whereas that of paraffin mass flow is the least significant.

Applicability analysis of gas quenching granulation

(a) Searching for the gas quenching operating parameters of blast furnace slag based on the similarity principle

In the gas-quenching granulation experiment, the fluid began to disperse upon jet-stream impact. The main factors that affect the granulation effect are air velocity, air flow, and the properties of the fluid, including density, viscosity, and surface tension. From the principles of dimensional analysis, π theorem, in reference [19], we can obtain the following similarity criteria:

$$\pi_1 = \frac{\upsilon_g}{\mu_1^{-2}\sigma_1} \tag{3}$$

$$\pi_2 = \frac{Q_g}{\rho_1^{-2}\mu_1^{2}\sigma_1^{-2}} \tag{4}$$

$$\pi_3 = \frac{q_1}{\rho_1^{-2}\mu_1^{2}\sigma_1^{-2}} \tag{5}$$

where ρ_l, μ_l, σ_l and q_l are the density, viscosity, surface tension and flow of the fluid, respectively; v_g and Q_g are the velocity and flow of air.

We assume that the parameters are ρ_l, μ_l, σ_l, q_l, v_g and Q_g to be the parameters when paraffin was granulated and ρ_l', μ_l', σ_l', q_l', v_g' and Q_g' to be the parameters when blast furnace slag was granulated. Therefore, $P_l' = C_\rho\rho_l$, $\sigma_l' = C\sigma\sigma_l$, $\mu_l' = C_\mu\mu_l$, $v_g' = C_v v_g$, $q_l' = C_q q_l$ and $Q_g' = C_Q Q_g$, where C is a proportionality constant, $\rho_l = 880$ kg/m^3, $\mu_l = 0.03$ Pa·s, $\sigma_l = 0.02$ N/m, $\rho_l' = 3000$ kg/m^3, $\sigma_l' = 0.5$ Pa·s and $\mu_l' = 0.55$ N/m.

The similarity criteria are equal. Hence, through eq. (3), we can obtain

$$\pi_1 = \frac{\upsilon_g}{\mu_1^{-2}-\sigma_1} = \frac{\upsilon_g'}{\mu_1'^{-2}-\sigma_1'} = \frac{c_v\upsilon_g}{c_u^{-2}\mu_1^{-2}c_\sigma\sigma_2}$$

Therefore, $\frac{\upsilon_g}{\mu_1^{-2}\sigma_1} = \frac{c_v}{c_u^{-2}c_\sigma} \times \frac{\upsilon_g}{\mu_1^{-2}\sigma_1}$, which indicates that

$$\frac{c_v}{c_u^{-2}c_\sigma} = 1 \tag{6}$$

Similarly, through eqs. (4) and (5) we can obtain

$$\frac{c_Q}{c_0^{-2}c_u^{2}c_\sigma^{-1}} = 1 \tag{7}$$

$$\frac{c_Q}{c_0^{-2}c_u^{2}c_\sigma^{-2}} = 1 \tag{8}$$

The phenomena and results of the gas quenching granulation experiment demonstrate that paraffin can be granulated under certain conditions, with a uniform particle size distribution of mostly 2 mm or less. The granulation process of blast furnace slag is similar to that of paraffin, and thus, blast furnace slag may also achieve the expected granulation effect under certain conditions.

Through eq. (6), we can obtain $C_v = \frac{c_\sigma}{c_\mu}$, which is $v_g = v_g\frac{c_\sigma}{c_\mu}$, and the optimal air velocity of the granulating paraffin is 57.7 m/s, and thus v_g' = 76.38 m/s. Through eq. (7) we can obtain $C_Q = \frac{c_u^2}{c_0^2 c_\sigma}$, which is

$Q_g = Q_g \frac{c_u^2}{c_0^2 c_\sigma}$, and the optimal air flow of the granulating paraffin is 8 m^3/h, and thus Q'_g = 151.11 m^3/h. Through eq. (8) we can obtain $C_q = \frac{c_u^2}{c_0^2 c_\sigma}$, which indicates that $q_l = q_l \frac{c_u^2}{c_0^2 c_\sigma}$, and the optimal liquid flow of the granulating paraffin is 23.65 L/h, and thus q'_1 = 446.72 L/h. Accordingly, we determine that the mass flow of blast furnace slag is 1340 kg/h, and the compressed air consumption is 0.11 m^3 per kilogram of slag.

(b) Estimation of energy consumption for granulating per unit mass of blast furnace slag

The energy consumption for granulating blast furnace slag with compressed air is mainly comes from the fan.

The formula for fan power is

$$P = Q \times p/(3600 \times 1000 \times \eta) \quad (9)$$

where P is the fan power in kW; Q is the air flow in m^3/h; p is the fan pressure in Pa; and η is the efficiency of the fan, which ranges from 0.75 to 0.85. We assume efficiency to be 0.8.

The parameters when blast furnace slag was granulated is determined in Section (a), *i.e.*, Q = Qg = 151.11 m^3/h and p = p′g = 0.60 MPa. Through eq. (9), we can estimate that the fan power consumed in granulating blast furnace slag is 26.23 kW. The energy consumption for granulating per kilogram of slag is 70.48 kJ, which is significantly less than the thermal energy per kilogram of contained slag (from 1260 kJ to 1880 kJ).

(c) Morphology of the gas quenching particles

The liquid granulated via compressed air is prone to the "drawing" phenomenon, particularly in the case of high air velocity. In this experiment, the morphology of the gas quenching particles under an air velocity of 57.7 m/s is shown in Fig. 12, and that morphology of the gas quenching particles under an air velocity of 113.2 m/s is shown in Fig. 13.

Fig. 12 Morphology of the gas quenching particles in air velocity of 57.7 m/s

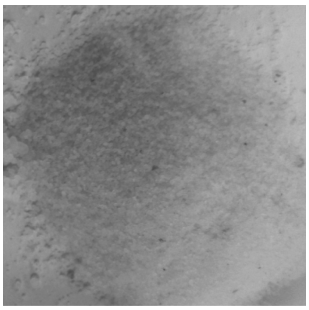

Fig. 13 Morphology of the gas quenching particles in air velocity of 113.2 m/s

The figures indicate that the granulation effect of paraffin particles obtained in this experiment is good. When air velocity was less than 113.2 m/s, the gas quenching particles did not exhibit the "drawing" phenomenon.

(d) Calculation of blast furnace slag drop height

If the solidification time of the blast furnace slag is calculated, then we confirm that the collected slags are solid particles when the drop height of the particles is greater than a certain value. We assume that the solidification temperature of blast furnace slag is 1573 K and determine the solidification time required when the slag is solidified from 1873 K.

Throughout the process, the film temperature of air in contact with the blast furnace slag was decreased, and the thermal conductivity of air was also reduced. Therefore, we selected the film temperature parameters at the end of solidification to ensure that the calculated solidification time will not be less than the actual solidification time.

The film temperature is (1573+293)/2 = 933 K, and the parameters of air at 933 K are k = 0.06525 W/(m·K) and υ = 0.0001082 m^2/s.

The parameters of granulating slags were obtained in Section (a), i.e., v'_g = 76.38 m/s. The particle size (D) of blast furnace slag ranged from 0.5 mm to 2 mm.

When the particle size is 0.5 mm, the Reynolds number is

$$Re = \frac{\upsilon'_g D}{\upsilon} = \frac{76.38 \times 0.0005}{0.0001082} = 353 \quad (10)$$

When the particle size is 2 mm, the Reynolds number is

$$Re = \frac{\upsilon'_g D}{\upsilon} = \frac{76.38 \times 0.002}{0.0001082} = 1411.83 \quad (11)$$

The Nusselt number (Nu) is

$$Nu = \frac{hD}{k} = 0.37\,Re^{0.6} \quad (12)$$

$$h = \frac{0.37k\,Re^{0.6}}{D} \quad (13)$$

When the particle size is 0.5 mm, the heat transfer coefficient is

$$h = 1631\,W/\left(m^2 \cdot K\right) \quad (14)$$

When the particle size is 2 mm, the heat transfer coefficient is

$$h = 937W/\left(m^2 \cdot K\right) \quad (15)$$

Surface area and volume can be determined according to particle size. The density of blast furnace slag is ρ = 3000 kg/m^3, the latent heat of solidification is 209000 J/kg, the specific heat is 1200 J/(kg·K), and the enthalpy loss during solidification can be obtained using eq. (16).

$$Q = (300 \times 1200 + 209000) \times 3000 \times \frac{4\pi}{3} \times (\frac{D}{2})^3 \quad (16)$$

When D is 0.5 mm, Q is 0.894 J. When D is 2 mm, Q is 57.202 J.

The blast furnace slag falling height is

$$L = \frac{gt^2}{2} \quad (17)$$

The solidification time is t = 0.136 s when D = 0.5 mm. At this time, the drop height is L = 0.09 m.

The solidification time is t = 0.949 s when D = 2 mm. At this time, the drop height is L= 4.5 m. When air velocity is $v_g^{'}$ = 76.38 m/s, all blast furnace slags can be solidified if the drop height is higher than 4.5 m.

Conclusions

(1) The average diameter of paraffin particles decreases with increasing air velocity. Moreover, the effects of air velocity gradually weaken with decreasing air velocity. When air velocity ranges from 30 m/s to 60 m/s, the effect of air velocity on the granulated diameter is more significant, and the curve of their relationship is approximately linear under the conditions used in the experiment. When air velocity is greater than 60 m/s, the granulation effect is weakened. Consequently, the curve gradually levels off.

(2) The granulation degree of the particle is gradually reduced with decreasing air flow, and the diameter of the particles increases. Under the conditions in the experiment, the particles with a diameter of <1 mm account for over 70% when air velocity is 113.2 m/s; the particles with a diameter of >1 mm reach approximately 50% when air velocity is 28.3 m/s. The impact force of air acting on a unit mass of liquid paraffin increases with gas-liquid mass ratio. The granulation effect increases with droplet formation. The granulation effect weakens with an increase in paraffin liquid column diameter. The relationship between liquid column diameter and gas quenching particle diameter is approximately linear.

(3) The effect of air velocity on particle diameter is the most significant, followed by those of air flow and liquid pipe diameter, whereas that of liquid mass flow is the least significant.

Acknowledgements

This study is supported by the National Natural Science Foundation of China (Grant No. 51206010) and the National Basic Research Program of China (973 Program) (Grant No. 2012CB720406).

References

[1] M. Barati, S. Esfahani, *et al*., Energy recovery from high temperature slags, *Energy*, 36 (2011), 9, pp. 5440−5449.

[2] G. Bisio. Energy recovery from molten slag and exploitation of the recovered energy, *Energy*, 22 (1997), 5, pp. 501−509.

[3] H.F. Wang, C.X. Zhang, *et al*., Quantitative analysis of non-crystalline and crystalline solids in blast furnace slag, *Journal of Iron and Steel Research*, International, 18 (2011), 1, pp. 8−10.

[4] S.J. Pickering, N. Hay, *et al*., New process for dry granulation and heat recovery from molten blast-furnace slag, *Ironmaking and Steelmaking*, 12(1985), 1, pp.14−20.

[5] N. Maruoka, T. Mizuochi, *et al*., Feasibility study for recovering waste heat in the steelmaking industry using a chemical recuperator, *Transactions of the Iron and Steel Institute of Japan*, 44 (2004), 2, pp. 257−262.

[6] Y. Min, J. Huang, *et al*., Physical Simulation of Molten Slag Granulation by Rotary Disk, *Journal of Iron and Steel Research*, International, 20 (2013), 9, pp. 26−32.

[7] H. Zhang, H. Wang, *et al*., A review of waste heat recovery technologies towards molten slag in steel industry, *Applied Energy*, 112 (2013), pp. 956−966.

[8] X. Liu, X. Zhu,*et al*., Theoretic analysis on transient solidification behaviors of a molten blast furnace slag particle, *CIESC Journal*, 65 (2014), S1, pp. 285−291.

[9] Y.J. Qiu, X. Zhu, *et al*., Three-dimensional simulation of solidification and heat transfer for air-cooling molten blast furnace slag droplet, *CIESC Journal*, 65 (2014), S1, pp. 340−345.

[10] D.J. Jiang, H.F. Liu, *et al*., Modeling atomization of a round water jet by a high-speed annular air jet based on the self-similarity of droplet breakup, *Chemical Engineering Research and Design*, 90 (2012), 2, pp. 185−192.

[11] A. Aliseda, E.J. Hopfinger, *et al*., Atomization of viscous and non-Newtonian liquids by a coaxial, high-speed gas jet. *Experiments and droplet size modeling, International Journal of Multiphase Flow*, 34 (2008), 2, pp. 161−175.

[12] J.F. Lou, T. Hong, *et al*., Numerical study on shearing breakup of liquid droplet in gas medium, *Chinese Journal of Computational Mechanics*, 28 (2011), 2, pp. 210−213.

[13] W.X. Li. Blast Granulation Technology for BOF Slag, Anhui Metallurgy, 2 (2009), 3, pp. 43−46.

[14] Y.Z. Zhang, Y. Long, *et al*., Application of Similarity Principle to Cold Simulation of Granulation of Steel Slag, *Journal of Northeastern University (Natural Science)*, 31 (2010), 2, pp. 207−209.

[15] Q.B. Yu, J.X. Liu, *et al*., Simulation Experimental Research of Granulation Process for Iron Slag, *Iron and Steel*, 44 (2009), 4, pp. 82−85.

[16] Y. Long, H.Y. Wei, *et al*., Simulation study of selection liquid slag treatment process, *Energy for Metallurgical Industry*, 29 (2010), 1, pp. 37−40.

[17] J. Liu, Q. Yu, *et al*., Experimental investigation on ligament formation for molten slag granulation, *Applied Thermal Engineering*, 73 (2014), 1, pp. 888−893.

[18] L.Ai, L.S. Shen, et al., Flow behavior of the 58°C paraffin oil, *Journal of Fushun Petroleum Institute*, 23 (2003), 1, pp. 29−32.

[19] X. J. Liu, Engineering Fluid Mechanics, *China Electric Power Press*, Beijing, 2007.